https://doi.org/10.5194/egusphere-2025-283
Preprint. Discussion started: 13 February 2025

Enhancement of near-inertial waves by cyclonic eddy in the northwestern South China Sea during spring 2022

Qi'an Chen[1,2], Hongzhou Xu[1*], Dongxiao Wang[3,4], Bo Hong[5*], Chunlei Liu[6,7,8], Zheyang Zhang[1], Huichang Jiang[1], Wei Song[3], Tong Long[1], Ling Wang[1,2], Sumin Liu[1], Rongjie Chen[1,2]

[1]Institute of Deep-sea Science and Engineering, Chinese Academy of Sciences, Sanya, 572000, China
[2]University of Chinese Academy of Sciences, Beijing, 100049, China
[3]School of Marine Sciences, Sun Yat-sen University, Zhuhai, 519000, China
[4]South Marine Science and Engineering Guangdong Laboratory (Zhuhai), Zhuhai, 519082, China
[5]School of Civil and Transportation Engineering, South China University of Technology, Guangzhou, 510641, China
[6]College of Ocean and Meteorology, Guangdong Ocean University, Zhanjiang, 524088, China
[7]South China Sea Institute of Marine Meteorology, Guangdong Ocean University, 529568, Zhanjiang, China
[8]CMA-GDOU Joint Laboratory for Marine Meteorology, Guangdong Ocean University, Zhanjiang, 524088, China

Correspondence to: Hongzhou Xu (Email: hzxu@idsse.ac.cn); Bo Hong (bohong@scut.edu.cn)

Abstract. By analyzing dataset derived from four moorings during spring 2022, this study provides direct evidence that near-inertial waves (NIWs) can be largely enhanced by a passing cyclonic eddy (CE) in the northwestern South China Sea. Results show that the enhancement of NIWs mainly occurred at north side of the CE due to asymmetry of eddy structure. In vertical, the enhancement concentrated at above 200 m and reached peaks at around 100 m. Significant energy transfer rates between the CE and NIWs appeared at the same depth of the enhancement that can reach up to 6×10^{-10} m^2/s^3 at the CE's edge. Under impact of the CE, power of the first five NIWs modes were promoted significantly and dominated by the second and third modes. Overall, the CE transferred energy to NIWs before near-inertial kinetic energy reaching its peaks, while NIWs gave energy back to the CE after the peaks.

1 Introduction

Near-inertial waves (NIWs) are ubiquitous features throughout the global ocean with frequencies near the Coriolis frequency *f* (Garrett, 2001). As dominant modes of high-frequency variability in oceans, they contain half of the kinetic energy in internal wave fields (Alford, 2003; Ferrari and

https://doi.org/10.5194/egusphere-2025-283
Preprint. Discussion started: 13 February 2025

Wunsch, 2009; Alford et al., 2016). NIWs transfer energy from mixed layer to interior and ultimately dissipate into microscale turbulent mixing, providing an energy source for abyssal diapycnal mixing (Ferrari and Wunsch, 2009; Chen et al., 2017). Therefore, NIWs are of vital importance for energy cascade among multiscale dynamic processes.

Due to horizontal spatial scales of 10–100 km and slow group speed of NIWs, they are likely to interact strongly with mesoscale eddy in oceans (Alford et al., 2016). Besides resonant frequency shifting from local f to the effective inertial frequency caused by mesoscale vorticity (Weller, 1982; Kunze, 1985; Klein et al., 2003), energy transfer between eddy and NIWs also plays an important role in oceanic energy cascade (Ferrari and Wunsch, 2009; Thomas, 2017). Researchers have stated that the NIWs can extract energy from eddy and affect the vertical transport (Barkan et al., 2021; Esposito et al., 2023). Moreover, enhanced wave dissipation near the critical layer balances the energy transfer from mean flows and conserve the near-inertial energy during eddy migration (Xu et al., 2022a).

Jing et al. (2017, 2018) suggested that permanent energy can be transferred from eddies to NIWs under a positive Okubo–Weiss parameter condition. Furthermore, Yu et al. (2022) revealed that enhanced near-inertial kinetic energy (NIKE) is found preferentially in regions of anticyclonic vorticity. Using surface drifter dataset, Liu et al. (2023) indicated that bidirectional energy transfer exists between eddy and NIWs in the global oceans. Above studies all emphasized role of eddy on affecting frequencies of NIWs, NIKE as well.

As the largest semi-enclosed marginal sea in the northwestern Pacific Ocean, the South China Sea (SCS) has frequent eddy activities (Wang et al., 2003; Wang et al., 2008; Chen et al., 2011; Nan et al., 2011; Chu et al., 2014). Using different eddy detection algorithms and criteria, many studies have statistically investigated the eddy number and mean properties (Wang et al., 2003; Lin et al., 2007; Xiu et al., 2010). Chen et al. (2011) suggest that eddies present 35%–60% of the time in the northern SCS, which play an important role in material transport and energy transfer (Zhang et al., 2015; He et al., 2018; Zhang et al., 2019; Liu et al., 2023; Zhang et al., 2023). Researchers have examined eddy properties (Wang et al., 2023; Zhao et al., 2023), eddy structures (Zhang et al., 2016; He et al., 2018; Chu et al., 2022) and energy exchange during eddy process in the SCS (Chu et al., 2014; Huang et al., 2018; Xu et al., 2022b; Liu et al., 2023; Zhang et al., 2023; Fan et al., 2024).

In the northwestern SCS, large portion of eddy propagate westward and terminate near Xisha Trough (Fig. 1a; Wang et al., 2003; Zhai et al., 2010), making this place as a seemly area for

https://doi.org/10.5194/egusphere-2025-283
Preprint. Discussion started: 13 February 2025

investigating NIWs and its interaction with eddy. However, interaction and energy exchange processes between them remain to be investigated in this area. In this study, four moorings equipped with Teledyne RD Acoustic Doppler Current Profiler (ADCP) instrument were deployed in the Xisha Trough of the northwestern SCS (Fig. 1a). During spring 2022, a cyclonic eddy (CE) propagated westward across the mooring array, giving an opportunity to study energy transfer between NIWs and the CE in this area. We introduce data and methods in Section 2, present observing results in Section 3, discuss energy transfer between NIWs and the CE in Section 4, and give a conclusion in Section 5.

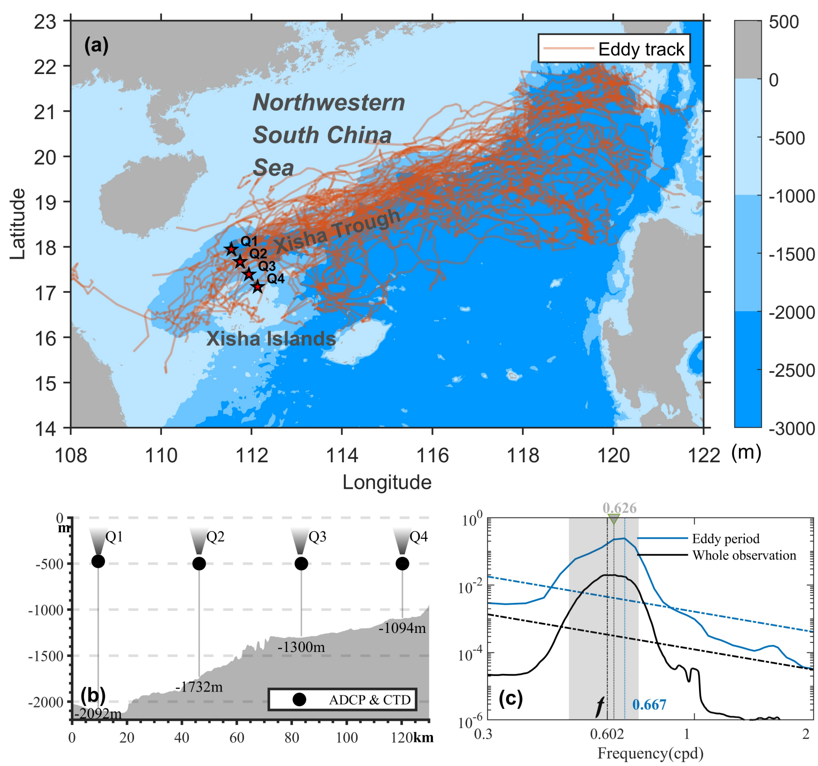

Figure 1: (a) Location of four moorings (Q1-Q4) in the northwestern SCS. The shaded background color represents topography. Orange lines indicate tracks of long-lasting eddy propagating from the Luzon area to the Xisha Trough from 1993 to 2023. **(b)** Structure of up-looking ADCP mooring along the slope of topography. **(c)** The power spectra during eddy period (blue line) and whole observation period (black line). The spectra are averaged at above 200 m.

https://doi.org/10.5194/egusphere-2025-283
Preprint. Discussion started: 13 February 2025

2 Methodology

2.1 Data

The four moorings (Q1-Q4) were deployed in the study area on August 21-23, 2021. One up-looking 75-kHz ADCP along with a CTD (SBE 37sm) was fixed at approximately 480 m depth and continuously monitored current velocity for each mooring (Fig. 1b). The ADCPs were set to have 30 bins with 16 m of vertical interval and 30 minutes of temporal interval, enabling extraction of NIWs of the upper ocean. The moorings were recovered on November 13-15, 2022. Several ADCP bins near sea surface were omitted due to large fluctuations, and the remaining were linearly interpolated vertically. Due to the significant vertical fluctuations based on CTD data in certain periods, flow velocity compensation correction was applied to ADCP data, which was calculated based on depth change and flow direction.

The Copernicus Marine Environment Monitoring Service (CMEMS) provides daily geostrophic current and sea level anomaly (SLA) data with a resolution of 0.25° × 0.25°, which were used to detect eddy during the observing period. The 1/12° three-dimensional products were obtained from CMEMS to calculate energy transfer rate between eddy and NIWs. The SLA dataset from Archiving, Validation, and Interpretation of Satellite Oceanographic (AVISO) was used to validate the existence of eddy and provide trajectory of eddy's center. World Ocean Atlas (WOA18) data was used to extract temperature and salinity data. The European Centre for Medium-Range Weather Forecasts (ECMWF) Reanalysis V5 (ERA-5) data, which has hourly temporal and 0.25° spatial resolutions, was used to calculate near-inertial energy input from the wind field.

2.2 Method

Eddy-NIWs energy transfer rate ε can be qualitatively calculated as (Jing et al., 2017):

$$\varepsilon = -\left(\langle u_i u_i\rangle - \langle v_i v_i\rangle\right)\frac{S_n}{2} - \langle u_i v_i\rangle S_s\,, \tag{1}$$

where $S_n = \frac{\partial u_g}{\partial x} - \frac{\partial v_g}{\partial y}$ and $S_s = \frac{\partial u_g}{\partial y} + \frac{\partial v_g}{\partial x}$ are the normal strain and shear strain of the geostrophic velocity u_g and v_g, which is obtained from the reanalysis data (Chen et al., 2023). We used fourth-order Butterworth band-pass filter with the cutoff frequency (0.8f-1.2f) to separate near-inertial velocity u_i and v_i. The $\langle\cdot\rangle$ represents a moving average of 3 internal tide periods.

https://doi.org/10.5194/egusphere-2025-283
Preprint. Discussion started: 13 February 2025

Near-inertial wind work was estimated as (Dasaro, 1985; Alford, 2001):

$$W = \vec{\tau} \cdot \vec{u}_i, \quad (2)$$

where $\vec{u}_i$ is near-inertial velocity at sea surface and $\vec{\tau}$ is wind stress calculated as (Liu et al., 2019; Alford, 2020):

$$\vec{\tau} = \rho_a C_D \left|\vec{U}_{10} - \vec{u}_c\right| \left(\vec{U}_{10} - \vec{u}_c\right), \quad (3)$$

where ρ_a=1.3kg/m^3 is density of air, $\vec{U}_{10}$ is 10-m wind velocity vector, $\vec{u}_c$ is ocean current vector, C_D is drag coefficient (Oey et al., 2006).

We used the Okubo-Weiss parameter (OW) (Provenzale, 1999) method to detect the CE. The OW method was computed from the horizontal velocity field as follows:

$$\sigma = S_{\mathrm{sh}}^2 + S_{\mathrm{st}}^2 - \zeta^2, \quad (4)$$

where S_{sh} and S_{st} are the shear and strain deformation, respectively, and ζ is the relative vorticity.

3 Results

3.1 Near inertial frequency and NIKE

The snapshots of SLA and surface geostrophic velocity fields show that the CE approached the mooring array on February 1 (Fig. 2). Its center passed through Q3 around February 26 and it left the mooring array on March 9. During the whole observation period, NIWs have a small blue shift of near-inertial frequency with peak value of 0.616 cpd (Fig. 1c). While a significant blue shift appeared during eddy period (February 1 - March 9) due to the background positive vorticity of the CE. The peak of spectral frequency (ω_{p}) reached 0.667cpd, with a relative frequency shift ($\frac{\omega_{\mathrm{p}}-f}{f}$, RFS) of about 10.8% in this area. It is significantly larger than the global RFS (Guo et al., 2021), suggesting significant impact of the CE on local near-inertial frequencies.

https://doi.org/10.5194/egusphere-2025-283
Preprint. Discussion started: 13 February 2025

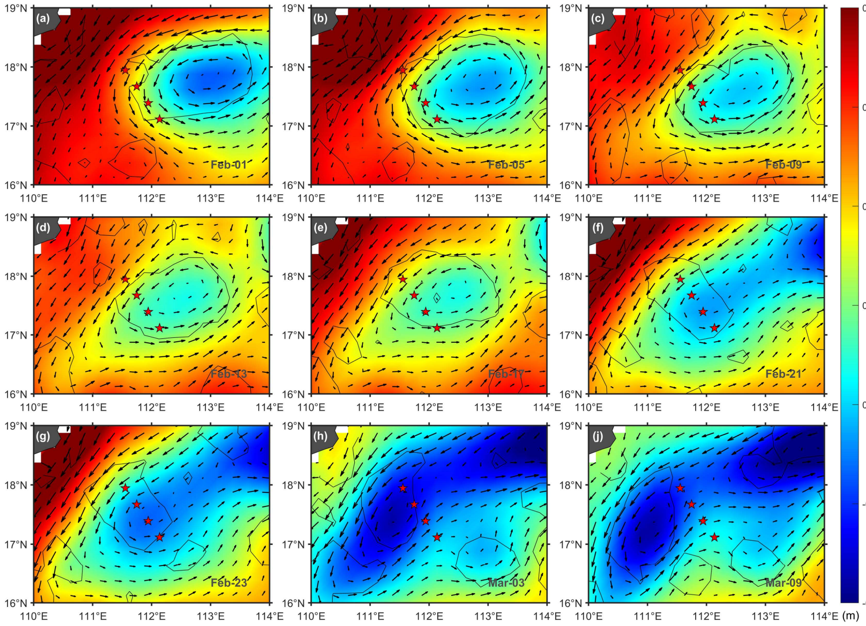

Figure 2: (a-j) The snapshot of sea level anomaly and geostrophic current vector during February 1-March 9. The black line indicates the Okubo-Weiss parameters.

Meridional velocity wavelet power spectra show that strong power of NIWs occurred during eddy period but with large variations at different eddy stages (Figs. 3a-d). To qualify NIKE at different stages of the CE, we defined two time periods named as Period1 (February 16-26) and Period2 (February 26-March 8), covering 10 days before and after the eddy's center passed through the mooring array. In addition, no eddy period with calm wind during June 1-20 was chosen for extra comparison. Figs. 3e-h show temporal and vertical variations of NIKE at the four moorings during eddy period. The absences of NIKE at surface layers are due to mooring swing caused by strong currents. It can be seen that NIKEs were enhanced largely at above 200 m during Period2. And peak values of NIKE concentrated at around 100 m. The time-averaged NIKEs during Period2 have almost one order larger than that during no eddy period (Figs. 3i-l), suggesting significant impact of the CE on local NIKE. Moreover, NIKEs illustrate asymmetry in spatial during eddy period (Figs. 3e-l). At north side of the CE (Q1-Q2), NIKEs became much stronger than that at south side of the CE (Q3 and Q4), especially at Q2 with a maximum value up to 12.0 J/m^3 (Fig. 3f), which has the same magnitude as the result observed by Xu et al. (2022a).

https://doi.org/10.5194/egusphere-2025-283
Preprint. Discussion started: 13 February 2025

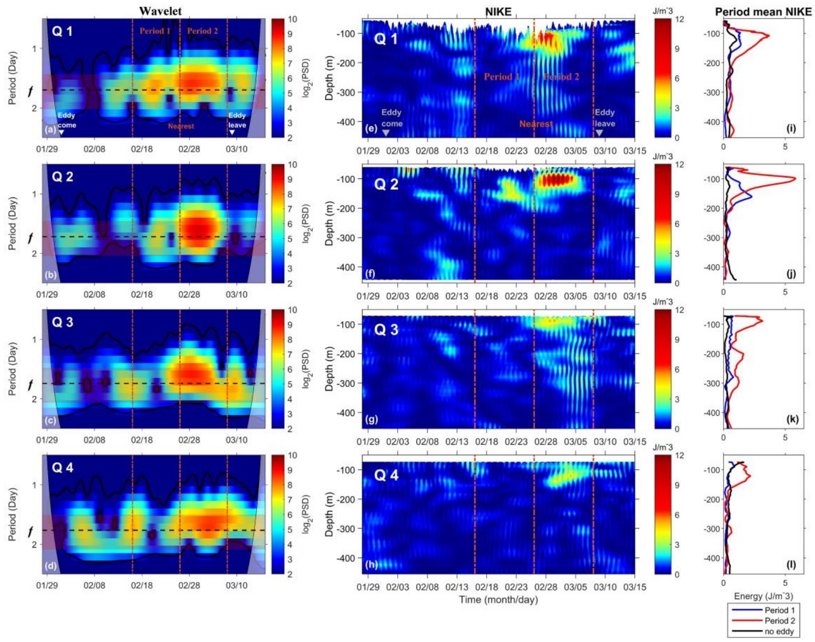

Figure 3: (a-d) 100 m-depth meridional velocity wavelet power spectra at Q1-Q4 during eddy period. **(e-h)** Vertical distribution of NIKE at Q1-Q4. The gray triangles indicate the time when the CE edge contacts and leaves the mooring array. **(i-l)** Vertical distribution of time-averaged NIKE during 'no eddy period' (black line), 'Period 1' (blue line), and 'Period 2' (red line) at Q1-Q4. The red dashed lines mark two periods of the CE.

3.2 Impact of eddy on NIWs

To ensure the fact that the CE could largely enhance NIWs in the northwestern SCS, we compared time series of vertical-integrated (above 200m) NIKE at each mooring with mooring-eddy distance, wind-input NIKE and eddy kinetic energy (EKE) in the study area (Fig. 4 and Fig. 5). NIWs were enhanced gradually accompanied by weakening EKE during Period1 when wind-input NIKE were relatively stable and minor. Results suggest a vivid energy transfer from eddy to NIWs during this period that will be qualified and discussed in Section 4. After passing of the CE's center, the CE enhanced NIWs faster, indicating more energy transfer from eddy to NIWs during Period2 than that during Period1. The slight increase of EKE during Period2 was contributed by background western boundary current velocity input (Fig. 1a).

https://doi.org/10.5194/egusphere-2025-283
Preprint. Discussion started: 13 February 2025

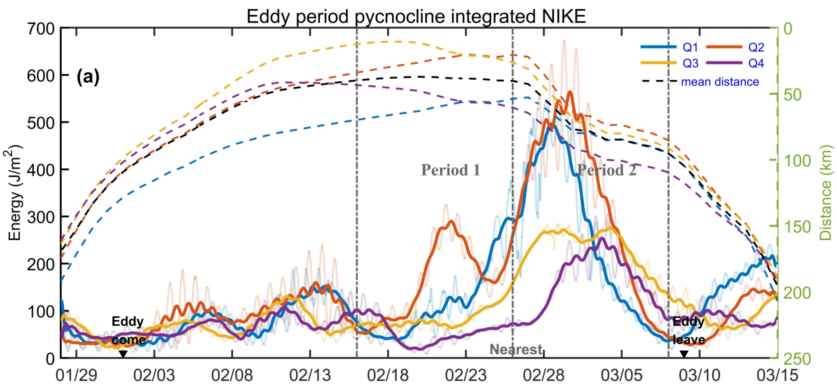

Figure 4: Time series of raw (thin lines) and daily-smoothed (thick lines) depth-integrated (above 200 m) NIKE at Q1-Q4 (solid lines) accompanying with distance between the CE's center and each mooring (dashed lines) during eddy period. The black dashed line represents the mean distance between the CE's center and four moorings. The triangles mark the time when the eddy edge contacts and leaves the mooring array.

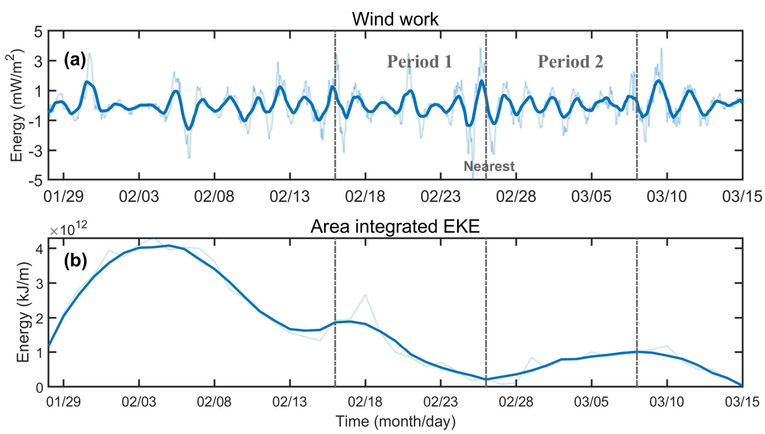

Figure 5: (a) Time series of raw (thin lines) and daily-smoothed (thick lines) averaged wind-input NIKE at Q1-Q4. **(b)** Time series of raw (thin lines) and daily-smoothed (thick lines) area integrated EKE.

In spatial, intensity of NIWs reached 600 J/ m² at Q2, while they merely had 300 J/m² at Q3 and Q4 due to vorticity asymmetry of the CE in which relative vorticities at north side (between Q1 and Q2) were much larger than those at south side (between Q3 and Q4) (Fig. 6). Zhao et al. (2021, 2023) pointed out that NIWs generation is significantly influenced by the eddy structure in which eddy with stronger shears tend to generate more powerful NIWs. In our case, the north side of the CE was merged with the western boundary current of the northwestern SCS (Fig. 1a) that generated strong shear and

https://doi.org/10.5194/egusphere-2025-283
Preprint. Discussion started: 13 February 2025

enhanced NIWs largely at this side.

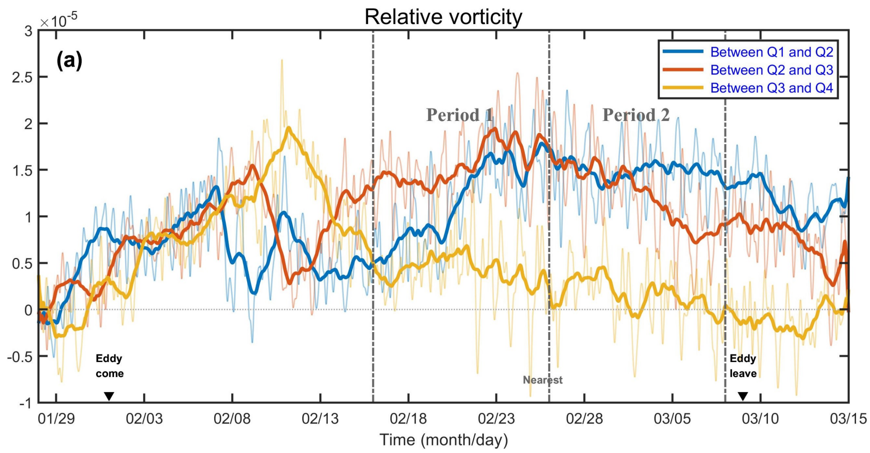

Figure 6: Time series of raw (thin lines) and daily-smoothed (thick lines) relative vorticity among four moorings. Vertical gray dashed lines mark two periods of the CE.

3.3 Impact of eddy on near-inertial modes

The CE not only affected frequency and energy of NIWs, but also their modes in the study area. Here, we calculated vertical-averaged energy (above 200 m) of the first five modes of near-inertial velocity during eddy period (Figs. 7a-d). All five modes grew since Period1 and reached peak values at Period2. But the CE has different influence on different modes with low modes (mainly the second and third modes) being significantly enhanced, especially near the CE's center. Low modes rose from 46% (Q2) and 54.4% (Q3) during Period1 to 87.6% (Q2) and 79.5% (Q3) during Period2, respectively (Figs 7e-f). The first mode has longer vertical wavelength and propagates faster than other modes that make it easy escape from eddy's influence (Chen et al., 2013). Overall, energy proportion of the first five modes were promoted from 81.5%, 66.8%, 69%, and 78.5% during Period1 to 90.8%, 88.8%, 87.7%, 94% at Q1-Q4, respectively (Figs. 7e-f), suggesting prominent influence of eddy on near-inertial modes in the northwestern SCS.

https://doi.org/10.5194/egusphere-2025-283
Preprint. Discussion started: 13 February 2025

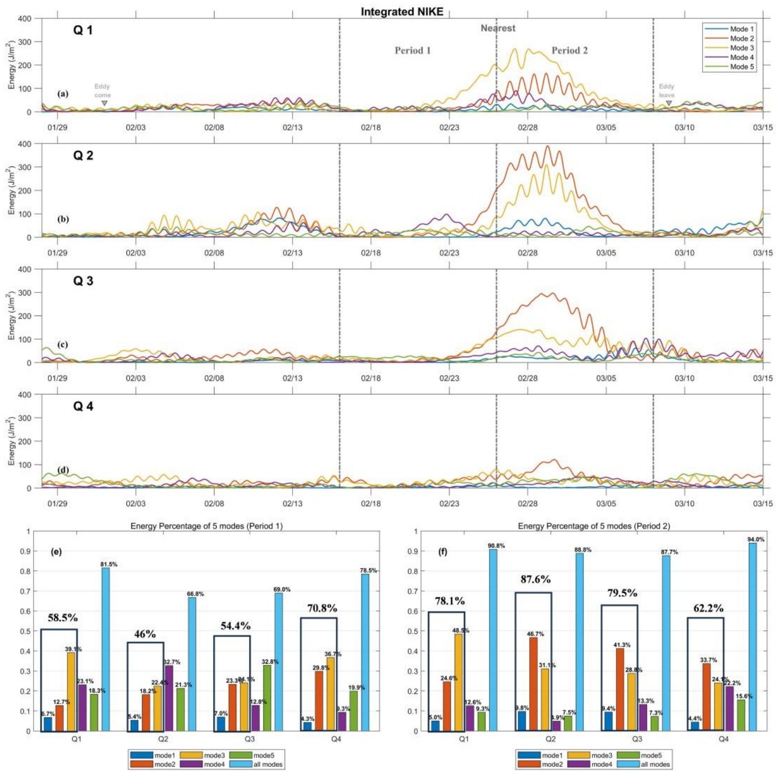

Figure 7： (a-d) Time series of NIKE for the first five modes at Q1-Q4 during eddy period. (e-f) The time-averaged proportions of each mode and all five modes during period 1 and period 2 at Q1-Q4. Black border indicates proportion sum of the first three modes.

4 Discussion

Energy exchange between eddy and NIWs is one of the most important processes in oceanic energy cascade (Ferrari and Wunsch, 2009; Alford et al., 2016; Thomas, 2017). By simulations, Jing et al. (2017) found that eddy-NIWs energy transfer efficiency is about 2% in Kuroshio Extension region. Based on surface drifter dataset, Liu et al. (2023) stated that energy transfer efficiency can reach about 13%, indicating previous underestimation of eddy impact on NIWs. For obtaining precise result, direct ocean current measurement by long-term mooring is essential (Jing et al., 2018). In this section, eddy-NIWs energy transfer rate during eddy period in the study area was qualified and discussed (Fig. 8). Corresponding to the layer of NIKE enhancement (Fig. 3), large energy transfer rates occurred at above 200 m with the peak values at around 100 m during eddy period, rather than surface and mixing layers (Jing et al., 2017; Liu et al., 2023). Both positive and negative transfer rates can reach a magnitude of 6

https://doi.org/10.5194/egusphere-2025-283
Preprint. Discussion started: 13 February 2025

$\times 10^{-10}$ m^2/s^3 in the study area, in which they are several times larger than the result of Jing et al. (2018), but they are smaller than Chen et al. (2023)'s result. The differences may be attributed to the strength of eddies, their rotation direction and the intensity of NIWs. In addition, eddy-NIWs energy transfer is largely dependent on eddy structure in which high rate can be caused by strong eddy shear (Zhao et al., 2023). It can be found that energy transfer at the CE's edge (Q1 and Q4) were more active than that at the CE's center (Q3). Although NIWs at Q4 were relative weak, the strong strains of the low frequency flow promoted local transfer rates at this area (Figs. 9a-b). Thomas and Daniel (2020) and Li et al. (2022) both stated that NIWS draw energy from background flow with small energy ratio between them, vice versa. Similarly, our results show that positive/negative energy transfers from the CE to NIWs dominated 'Before Strongest'/'After Strongest' periods at most mooring stations (Fig. 9c), indicating an inhomogeneous and bidirectional energy transfer between eddy and NIWs during different periods in the northwestern SCS.

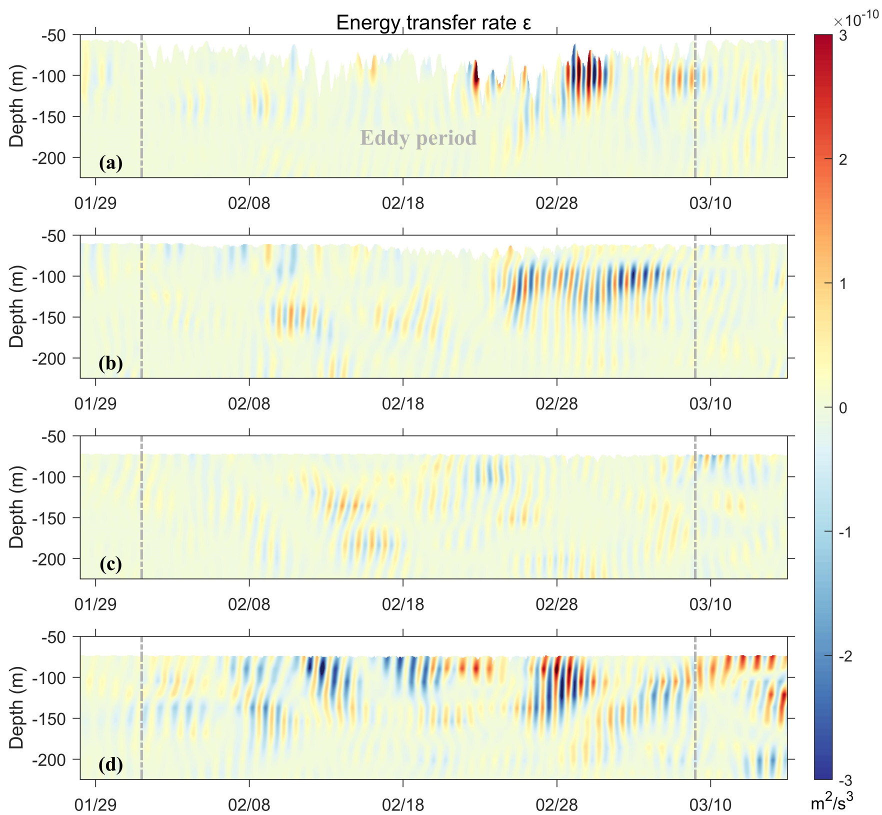

https://doi.org/10.5194/egusphere-2025-283
Preprint. Discussion started: 13 February 2025

Figure 8: (a-d) Vertical distribution of energy transfer rate between the CE and NIWs at Q1-Q4 during eddy period.

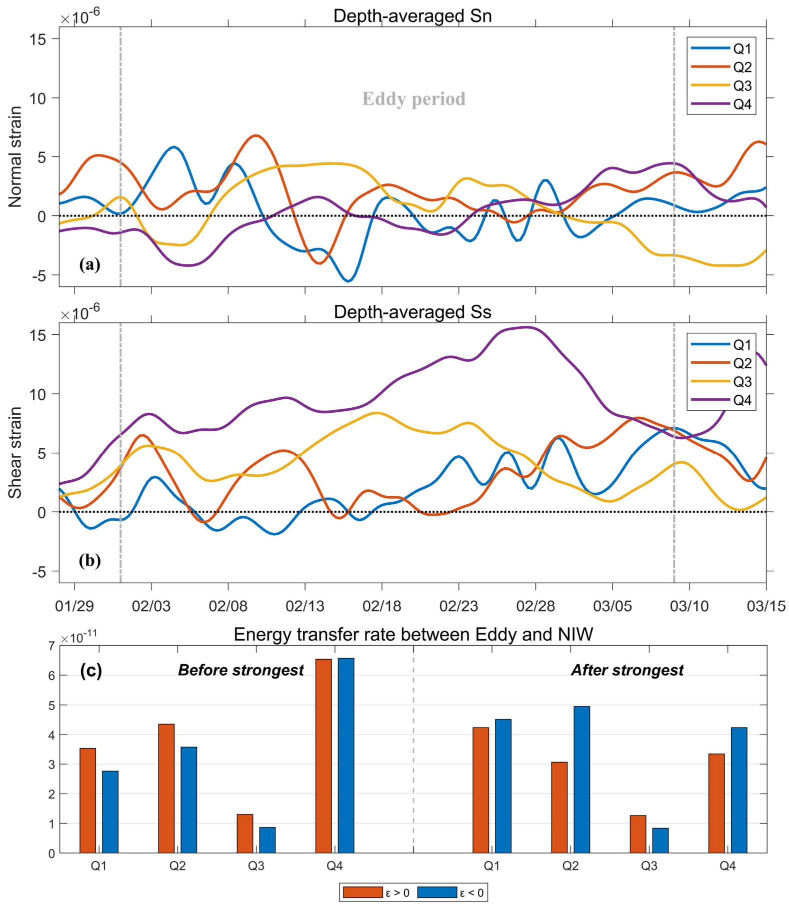

Figure 9: (a) Time series of depth-averaged (above 200 m) normal strain of the CE for each mooring. **(b)** Time-series of depth-averaged (above 200 m) shear strain of the CE for each mooring. **(c)** Time- (7 days) and depth-averaged (above 200 m) positive and negative energy transfer rates before and after the NIKE reaching its peak at Q1-Q4.

5 Conclusion

During spring 2022, the CE passed through the northwestern SCS. Our four long-term moorings with ADCP instruments captured the interaction and energy exchange processes between eddy and local NIWs for the first time in this area. We found that NIWs can be largely enhanced by the passing CE. Horizontally, the CE transferred more energy to NIWs at the north side than that at the south side

https://doi.org/10.5194/egusphere-2025-283
Preprint. Discussion started: 13 February 2025

of the CE due to asymmetry of eddy structure and strong shear. In vertical, the enhancement of NIKE occurred at above 200 m, with a maximum exceeding 12 J/m^3 at a depth of 100 m. Power comparison of different NIWs modes during eddy period indicate that the CE promoted percentage of first five modes, especially the second and third modes. Overall, NIWs drew energy from the CE during the enhancing period of NIKE, while they gave energy back to the CE during weakening period of NIKE. This study is helpful for us to understand multi-scale interaction and energy cascade in the northwestern SCS.

Data availability. The CMEMS products are available at https://data.marine.copernicus.eu/product/GLOBAL_MULTIYEAR_PHY_001_030/services. The ERA-5 wind data are available at https://doi.org/10.24381/cds.adbb2d47. The WOA2018 climatological monthly mean mixed layer depth data are available at https://www.ncei.noaa.gov/access/world-ocean-atlas-2018/. The AVISO eddy data are available at https://www.aviso.altimetry.fr/en/data/products/value-added-products/global-mesoscale-eddy-trajectory-product.html. The bathymetric data is from GEBCO Gridded Bathymetry Data (https://download.gebco.net). The mooring dataset used for plotting Figure for this paper are available at: https://10.5281/zenodo.14638959.

Author Contribution. H.Z.X. and B.H. conceived the central idea. Q.A.C. and H.Z.X. conducted most of the analyses and generated the Figures. Q.A.C., B.H. and H.Z.X. wrote the main manuscript. D.X.W, C.L.L, Z.Y.Z., H.C.J. contributed to the revision of the manuscript. H.Z.X., Z.Y.Z., H.C.J., W.S., T.L., L.W, S.M.L. and R.JC. conducted observations of the Mooring Array and participated in data analysis.

Competing interests. The contact author has declared that none of the authors has any competing interests.

Acknowledgments. This research is supported by Hainan Provincial Natural Science Foundation of China (Grant No. 423RC547), the National Natural Science Foundation of China (Grant No. 42376023, 42176033), the Natural Science Foundation of Guangdong Province (Grant No. 2024A1515012218 and 2022A1515011736), the Innovational Fund for Scientific and Technological Personnel of Hainan Province (Grant No. KJRC2023D39), and the Youth Innovation Promotion Association CAS (Grant No. 2022373).

https://doi.org/10.5194/egusphere-2025-283
Preprint. Discussion started: 13 February 2025

References

Alford, M. H.: Internal Swell Generation: The Spatial Distribution of Energy Flux from the Wind to Mixed Layer Near-Inertial Motions, Journal of Physical Oceanography, 31, 2359-2368, 2001.

Alford, M. H.: Redistribution of energy available for ocean mixing by long-range propagation of internal waves, Nature, 423, 159-162, 2003.

Alford, M. H.: Revisiting Near-Inertial Wind Work: Slab Models, Relative Stress, and Mixed Layer Deepening, Journal of Physical Oceanography, 50, 3141-3156, 2020.

Alford, M. H., MacKinnon, J. A., Simmons, H. L., and Nash, J. D.: Near-Inertial Internal Gravity Waves in the Ocean, Annual Review of Marine Science, 8, 95-123, 2016.

Barkan, R., Srinivasan, K., Yang, L., McWilliams, J. C., Gula, J., and Vic, C.: Oceanic Mesoscale Eddy Depletion Catalyzed by Internal Waves, Geophysical Research Letters, 48, e2021GL094376, 2021.

Chen, G., Hou, Y., and Chu, X.: Mesoscale eddies in the South China Sea: Mean properties, spatiotemporal variability, and impact on thermohaline structure, Journal of Geophysical Research, 116, 2011.

Chen, G., Xue, H., Wang, D., and Xie, Q.: Observed near-inertial kinetic energy in the northwestern South China Sea, Journal of Geophysical Research: Oceans, 118, 4965-4977, 2013.

Chen, S., Chen, D., and Xing, J.: A study on some basic features of inertial oscillations and near-inertial internal waves, Ocean Sci., 13, 829-836, 2017.

Chen, Z., Yu, F., Chen, Z., Wang, J., Nan, F., Ren, Q., Hu, Y., Cao, A., and Zheng, T.: Downward Propagation and Trapping of Near-Inertial Waves by a Westward-Moving Anticyclonic Eddy in the Subtropical Northwestern Pacific Ocean, Journal of Physical Oceanography, 53, 2105-2120, 2023.

Chu, F., Si, Z., Yan, X., Liu, Z., Yu, J., and Pang, C.: Physical structure and evolution of a cyclonic eddy in the Northern South China sea, Deep Sea Research Part I: Oceanographic Research Papers, 189, 2022.

Chu, X., Xue, H., Qi, Y., Chen, G., Mao, Q., Wang, D., and Chai, F.: An exceptional anticyclonic eddy in the South China Sea in 2010, Journal of Geophysical Research: Oceans, 119, 881-897, 2014.

Dasaro, E. A.: The Energy Flux from the Wind to near-Inertial Motions in the Surface Mixed Layer, Journal of Physical Oceanography, 15, 1043-1059, 1985.

Esposito, G., Donnet, S., Berta, M., Shcherbina, A. Y., Freilich, M., Centurioni, L., D'Asaro, E. A., Farrar, J. T., Johnston, T. M. S., Mahadevan, A., Özgökmen, T., Pascual, A., Poulain, P.-M., Ruiz, S., Tarry, D. R., and Griffa, A.: Inertial Oscillations and Frontal Processes in an Alboran Sea Jet: Effects on Divergence and Vertical Transport, Journal of Geophysical Research: Oceans, 128, e2022JC019004, 2023.

Fan, L., Sun, H., Yang, Q., and Li, J.: Numerical investigation of interaction between anticyclonic eddy and semidiurnal internal tide in the northeastern South China Sea, Ocean Science, 20, 241-264, 2024.

Ferrari, R. and Wunsch, C.: Ocean Circulation Kinetic Energy: Reservoirs, Sources, and Sinks, Annual Review of Fluid Mechanics, 41, 253-282, 2009.

Garrett, C.: What is the "near-inertial" band and why is it different from the rest of the internal wave spectrum?, Journal of Physical Oceanography, 31, 962-971, 2001.

Guo, M., Chen, R., Xu, H., and Vetter, P. A.: Dynamical features of near-inertial motions in global ocean based on the GDP dataset from 2000 to 2019, Acta Oceanologica Sinica, 40, 126-134, 2021.

He, Q., Zhan, H., Cai, S., He, Y., Huang, G., and Zhan, W.: A New Assessment of Mesoscale Eddies in the South China Sea: Surface Features, Three-Dimensional Structures, and Thermohaline Transports, Journal of Geophysical Research: Oceans, 123, 4906-4929, 2018.

https://doi.org/10.5194/egusphere-2025-283
Preprint. Discussion started: 13 February 2025

Huang, X., Wang, Z., Zhang, Z., Yang, Y., Zhou, C., Yang, Q., Zhao, W., and Tian, J.: Role of Mesoscale Eddies in Modulating the Semidiurnal Internal Tide: Observation Results in the Northern South China Sea, Journal of Physical Oceanography, 48, 1749-1770, 2018.

Jing, Z., Chang, P., DiMarco, S. F., and Wu, L.: Observed Energy Exchange between Low-Frequency Flows and Internal Waves in the Gulf of Mexico, Journal of Physical Oceanography, 48, 995-1008, 2018.

Jing, Z., Wu, L., and Ma, X.: Energy Exchange between the Mesoscale Oceanic Eddies and Wind-Forced Near-Inertial Oscillations, Journal of Physical Oceanography, 47, 721-733, 2017.

Klein, P., Hua, B. L., and Carton, X.: Emergence of cyclonic structures due to the interaction between near-inertial oscillations and mesoscale eddies, Quarterly Journal of the Royal Meteorological Society, 129, 2513-2525, 2003.

Kunze, E.: Near-Inertial Wave Propagation In Geostrophic Shear, Journal of Physical Oceanography, 15, 544-565, 1985.

Li, Q., Chen, Z., Guan, S., Yang, H., Jing, Z., Liu, Y., Sun, B., and Wu, L.: Enhanced Near-Inertial Waves and Turbulent Diapycnal Mixing Observed in a Cold- and Warm-Core Eddy in the Kuroshio Extension Region, Journal of Physical Oceanography, 52, 1849-1866, 2022.

Lin, P., Fang, W., Chen, Y., and Tang, X.: Temporal and spatial variation characteristics on eddies in the South China Sea I. Statistical analyses, Acta Oceanologica Sinica, 29, 14-22, 2007.

Liu, G., Chen, Z., Lu, H., Liu, Z., Zhang, Q., He, Q., He, Y., Xu, J., Gong, Y., and Cai, S.: Energy Transfer Between Mesoscale Eddies and Near‐Inertial Waves From Surface Drifter Observations, Geophysical Research Letters, 50, 2023.

Liu, Y., Jing, Z., and Wu, L.: Wind Power on Oceanic Near‐Inertial Oscillations in the Global Ocean Estimated From Surface Drifters, Geophysical Research Letters, 46, 2647-2653, 2019.

Nan, F., Xue, H., Xiu, P., Chai, F., Shi, M., and Guo, P.: Oceanic eddy formation and propagation southwest of Taiwan, Journal of Geophysical Research: Oceans, 116, 2011.

Oey, L. Y., Ezer, T., Wang, D. P., Fan, S. J., and Yin, X. Q.: Loop Current warming by Hurricane Wilma, Geophysical Research Letters, 33, 2006.

Provenzale, A.: Transport by Coherent Barotropic Vortices, Annual Review of Fluid Mechanics, 31, 55-93, 1999.

Thomas, J. and Daniel, D.: Turbulent exchanges between near-inertial waves and balanced flows, Journal of Fluid Mechanics, 902, 2020.

Thomas, L. N.: On the modifications of near-inertial waves at fronts: implications for energy transfer across scales, Ocean Dynamics, 67, 1335-1350, 2017.

Wang, G., Chen, D., and Su, J.: Winter Eddy Genesis in the Eastern South China Sea due to Orographic Wind Jets, Journal of Physical Oceanography, 38, 726-732, 2008.

Wang, G., Su, J., and Chu, P. C.: Mesoscale eddies in the South China Sea observed with altimeter data, Geophysical Research Letters, 30, 2003.

Wang, X., Du, Y., Zhang, Y., Wang, T., Wang, M., and Jing, Z.: Subsurface Anticyclonic Eddy Transited from Kuroshio Shedding Eddy in the Northern South China Sea, Journal of Physical Oceanography, 53, 841-861, 2023.

Weller, R. A.: The Relation of Near-Inertial Motions Observed in the Mixed layer During the JASIN (1978) Experiment to the Local Wind Stress and to the Quasi-Geostrophic Flow Field, Journal of Physical Oceanography, 12, 1122-1136, 1982.

Xiu, P., Chai, F., Shi, L., Xue, H., and Chao, Y.: A census of eddy activities in the South China Sea

https://doi.org/10.5194/egusphere-2025-283
Preprint. Discussion started: 13 February 2025

during 1993–2007, Journal of Geophysical Research: Oceans, 115, 2010.

Xu, H., Zhang, Z., Vetter, P. A., Xie, Q., Long, T., and Hong, B.: Impact of Anticyclonic Eddy on Nonlinear Wave - Wave Interaction in the Southern South China Sea During Late Summer 2020, Geophysical Research Letters, 49, 2022b.

Xu, X., Zhao, W., Huang, X., Hu, Q., Guan, S., Zhou, C., and Tian, J.: Observed Near-Inertial Waves Trapped in a Propagating Anticyclonic Eddy, Journal of Physical Oceanography, 52, 2029-2047, 2022b.

Yu, X., Naveira Garabato, A. C., Vic, C., Gula, J., Savage, A. C., Wang, J., Waterhouse, A. F., and MacKinnon, J. A.: Observed Equatorward Propagation and Chimney Effect of Near - Inertial Waves in the Midlatitude Ocean, Geophysical Research Letters, 49, 2022.

Zhai, X., Johnson, H. L., and Marshall, D. P.: Significant sink of ocean-eddy energy near western boundaries, Nature Geoscience, 3, 608-612, 2010.

Zhang, W. Z., Xue, H., Chai, F., and Ni, Q.: Dynamical processes within an anticyclonic eddy revealed from Argo floats, Geophysical Research Letters, 42, 2342-2350, 2015.

Zhang, Z., Liu, Y., Qiu, B., Luo, Y., Cai, W., Yuan, Q., Liu, Y., Zhang, H., Liu, H., Miao, M., Zhang, J., Zhao, W., and Tian, J.: Submesoscale inverse energy cascade enhances Southern Ocean eddy heat transport, Nature Communications, 14, 2023.

Zhang, Z., Liu, Z., Richards, K., Shang, G., Zhao, W., Tian, J., Huang, X., and Zhou, C.: Elevated Diapycnal Mixing by a Subthermocline Eddy in the Western Equatorial Pacific, Geophysical Research Letters, 46, 2628-2636, 2019.

Zhang, Z., Tian, J., Qiu, B., Zhao, W., Chang, P., Wu, D., and Wan, X.: Observed 3D Structure, Generation, and Dissipation of Oceanic Mesoscale Eddies in the South China Sea, Scientific Reports, 6, 2016.

Zhao, B., Liu, Z., Xu, Z., Yin, B., and Zheng, Q.: Spontaneous near-inertial wave generation from mesoscale eddy: Nonlinear forcing mechanism, Physics of Fluids, 35, 2023.

Zhao, B., Xu, Z., Li, Q., Min, W., Wang, Y., and Yin, B.: The characteristics of spontaneous near-inertial wave generation from an anticyclonic mesoscale eddy, Journal of Oceanology and Limnology, 40, 413-427, 2021.